Inorganic Chemistry

Article

pubs.acs.org/IC

Highly Uniform α-$NaYF_4$:Yb/Er Hollow Microspheres and Their Application as Drug Carrier

Yunhua Han,[†,‡] Shili Gai,*[,†] Ping'an Ma,[§] Liuzhen Wang,[†] Milin Zhang,[†] Shaohua Huang,[†] and Piaoping Yang*[,†]

[†]Key Laboratory of Superlight Materials and Surface Technology, Ministry of Education, Harbin Engineering University, Harbin 150001, P. R. China

[‡]Jilin Institute of Chemical Engineering, Jilin 132022, P. R. China

[§]State Key Laboratory of Rare Earth Resource Utilization, Changchun Institute of Applied Chemistry, Chinese Academy of Sciences, Changchun 130023, P. R. China

Supporting Information

ABSTRACT: Highly uniform α-$NaYF_4$:Yb/Er hollow microspheres have been successfully prepared via a simple two-step route. First, the core−shell structured MF@$Y(OH)CO_3$:Yb/Er precursor was fabricated by a urea-based homogeneous precipitation method using colloidal melamine formaldehyde (MF) microspheres as template. Then the $Y(OH)CO_3$:Yb/Er precursor was transformed into hollow $NaYF_4$:Yb/Er (α and β mixed phase) by a subsequent solvothermal method, and MF microspheres were dissolved in the solvent simultaneously. The mixed phase of $NaYF_4$:Yb/Er was transferred into pure α-$NaYF_4$:Yb/Er by calcination. The as-prepared hollow microspheres were well characterized by X-ray diffraction (XRD), scanning electron microscopy (SEM), transmission electron microscopy (TEM), energy-dispersive X-ray spectrum (EDS), Fourier transform infrared spectroscopy (FT-IR), thermogravimetric analysis (TGA), and upconversion (UC) luminescence spectroscopy. It is found that the template can be removed without additional calcination or etching process. α-$NaYF_4$:Yb/Er hollow microspheres exhibit bright upconversion (UC) luminescence under 980 nm laser diode (LD) excitation. Furthermore, the hollow microspheres show sustained and pH-dependent doxorubicin hydrochloride (DOX) release properties; in particular, the emission intensity increases with the release amount of drug, making the release process able to be tracked or monitored by the change of the emission intensity, which demonstrates the high potential of this kind of hollow fluorescent material in drug delivery fields.

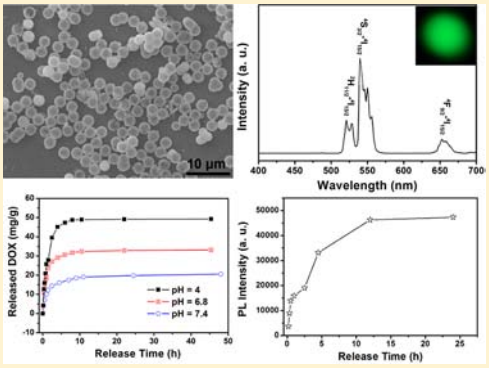

INTRODUCTION

In modern chemistry and materials science, controlled synthesis of uniform hollow nano- or microspheres has been a focus of worldwide research work, since hollow structure materials hold higher specific surface area, lower effective density, low refractive index, and better permeation. Thereby, hollow structured materials possess widespread potential applications in many fields, including drug-delivery carriers, efficient catalysts, adsorbents, sensors, photonic crystals, biomedical diagnosis agents, waste removal, and chemical reactors.[1−7] Hollow structures have gained special attention in the field of drug storage and release, because they simultaneously possess large voids inside the shells and mesopores at the shells.[8−10] The large voids can store more drug molecules than conventional mesoporous materials,[10] and mesopores at the shells can provide accessible channels for drug molecules diffusion and mass transfer without blocking. Meanwhile, they can also control the permeability of the shells for matter exchange between voids and the outer environment. The synthetic strategies for hollow structures can be broadly categorized into template and template-free approaches. In addition, the template method is the most common method for synthesizing hollow micro- and nanostructures. Generally, the template can be divided into soft template and hard template. Emulsion drops, polymer vesicles, surfactant micelle, polymer aggregates, and gas bubbles have been utilized as soft templates.[11−15] However, it is usually hard to control the dispersity and morphology of the hollow structures in soft template-based strategy due to the deformability of the soft templates. Compared with the soft template-based strategy, the hard template strategy is an effective approach to prepare hollow spheres with well-defined shape and good dispersity. In the hard template strategy, many compounds, such as polymeric (polystyrene,[16] poly(methyl methacrylate),[17−19] MF[20]), inorganic nonmetallic (SiO_2,[21−25] carbon spheres,[26] $CaCO_3$[27]), and metallic particles (Au[28]), have been extensively used as templates. In addition, the desired materials can be

Received: January 24, 2013
Published: July 30, 2013

   dx.doi.org/10.1021/ic4001818 | Inorg. Chem. 2013, 52, 9184−9191

coated on the templates to form core−shell structured spheres. Subsequently, the templates are removed by calcination at elevated temperature in air or by selective etching with a solvent to generate hollow structured spheres.

Currently, lanthanide-doped UC luminescent materials have gained considerable attention due to their superior chemical and optical properties, such as large Stokes shifts, multicolor emission, high resistance to photobleaching, and photochemical degradation.[29−37] Among various lanthanide-doped compounds, rare-earth fluoride with various morphologies are of special interest because they normally possess a high refractive index and low phonon energy.[38−40] Furthermore, they exhibit adequate thermal and environmental stability and therefore are regarded as excellent host lattices for UC luminescence of lanthanide ions.[41−44] In particular, cubic (α-) or hexagonal (β-) $NaYF_4$ has been reported as one of the most efficient infrared-to-visible UC fluorescent host materials.[45] To date, many methods have been developed to synthesize $NaYF_4$ crystals with various sizes and shapes. For instance, $NaYF_4$ nanocrystals have been made through hydrothermal or solvothermal processes,[46−52] solid treatment,[53] coprecipitation in aqueous phase,[54,55] and thermal decomposition of trifluoroacetate precursors.[56,57] However, to the best of our knowledge, only a few researchers have reported the synthesis of $NaYF_4$ hollow spheres. Zhang et al. prepared cubic $NaYF_4$ hollow spheres through a controlled ion-exchange process from solid Y_2O_3 spheres using HF acid as fluoride source.[58] Yang et al. employed a similar route to prepare $NaYF_4$ hollow spheres using lanthanide-doped $Y(OH)CO_3$ spheres as precursor.[59] However, the used corrosive acid often brings environmental concern, and the spheres prepared from the ion-exchange route lack high uniformity. As mentioned above, although some kinds of well-defined hollow spheres can be prepared using the hard template strategy, the template particles usually need to be removed by calcination or an etching process, resulting in a complicated process and enhanced energy consumption. Therefore, it is highly desirable to develop a cheap and environmentally friendly strategy to prepare well-defined and uniform $NaYF_4$ hollow spheres without an additional template removal process. In addition, hollow structures generally possess large voids inside the shells and small pores or broken holes at the shells and have great potential in the field of drug delivery. First, the large voids can store more drug molecules than that of the conventional porous materials. Second, the small pores or broken holes at the shells, on the one hand, can provide accessible channels for drug molecules diffusion and mass transfer without blocking and, on the other hand, could control the permeability of the shells for matter exchange between voids and the outer environment. In particular, the excellent UC luminescent properties of Yb^{3+}/Er^{3+}-codoped $NaYF_4$ make them a real-time, a simple, and an effective way to monitor the route of drug-transport carriers in a living system. In addition, the near-infrared excitation light offers high excitation-penetration depth and negligible photodamage. Therefore, $NaYF_4$ hollow structures as drug delivery systems can be easily identified, tracked, and monitored to evaluate the efficiency of drug release and disease therapy.

In this study, Yb^{3+}/Er^{3+}-codoped α-$NaYF_4$ (denoted as α-$NaYF_4$:Yb/Er) hollow microspheres with UC emission property have been fabricated through a two-step approach. Core−shell structured MF@$Y(OH)CO_3$:Yb/Er microspheres were first fabricated by a urea-based homogeneous precipitation method using colloidal MF microspheres as template. Then MF@$Y(OH)CO_3$:Yb/Er was transformed into $NaYF_4$:Yb/Er hollow microspheres by a subsequent solvothermal process, and MF cores were dissolved in the solvothermal process. After calcination, α-$NaYF_4$:Yb/Er hollow microspheres were obtained. Although the UC efficiency of the hexagonal form is about an order of magnitude higher than that of the cubic one, β-$NaYF_4$ can only be formed under drastic experimental conditions, such as high temperatures, high pressure, and high Na/Y ratio unfortunately, which are not beneficial to formation of hollow structures. The structure, formation process, UC luminescence properties, and drug release properties using doxorubicin hydrochloride (DOX) as a model drug of the hollow microspheres have been investigated in detail.

EXPERIMENTAL SECTION

Materials. All materials including Y_2O_3, Yb_2O_3, Er_2O_3, urea, formaldehyde, melamine, and formic acid were purchased from Sinopharm Chemical Reagent Co., Ltd. $Y(NO_3)_3$, $Yb(NO_3)_3$, and $Er(NO_3)_3$ were prepared by dissolving Y_2O_3, Yb_2O_3, and Er_2O_3 in dilute HNO_3 solution under heating and agitation. The superfluous HNO_3 was driven off by heating until the pH value of the solution reached between 3 and 4. All other chemicals were analytical-grade reagents and used directly without further purification.

Synthesis of Monodisperse MF Microspheres. Monodisperse MF colloidal microspheres were prepared according to the literature with a slight modification.[60] In a typical procedure, a solution containing 4.25 mL of formaldehyde (37%) and 80 mL of deionized water was heated to 80 °C. Subsequently, 1.0 g of melamine was added into the solution with stirring. When melamine was dissolved completely, formic acid was then introduced into the solution with vigorous stirring until reaching pH = 5. The transparent solution was further stirred for several minutes and then became turbid. After additional agitation for another 40 min, the obtained white colloidal particles were washed with deionized water and ethanol several times and dried in air at 60 °C for 12 h.

Preparation of MF@$Y(OH)CO_3$:Yb/Er Microspheres. Typically, 1.6 mmol of $Y(NO_3)_3$, 0.36 mmol of $Yb(NO_3)_3$, and 0.04 mmol of $Er(NO_3)_3$ were added to 30 mL of distilled water. Then 3.0 g of urea was dissolved in the solution with vigorous stirring to form a clear solution. Subsequently, 0.2 g of as-prepared MF microspheres was added and well dispersed into the above solution with the assistance of ultrasonication for 30 min. Finally, the mixture was transferred to a round-bottomed flask and heated to 85 °C for 3 h with vigorous stirring before the product was collected by centrifugation. Then as-obtained MF@$Y_{0.8}Yb_{0.18}Er_{0.02}(OH)CO_3$, also denoted as MF@$Y(OH)CO_3$:Yb/Er, microspheres was washed with deionized water and ethanol several times. To confirm formation of $Y_{0.8}Yb_{0.18}Er_{0.02}(OH)CO_3$ on the surface of MF, the experiment and results without the presence of MF as template are shown in the Supporting Information.

Synthesis of α-$NaYF_4$:Yb/Er Hollow Microspheres. In a typical process for the synthesis of α-$NaYF_4$:Yb/Er hollow microspheres, the as-obtained MF@$Y(OH)CO_3$:Yb/Er was dispersed into 15 mL of deionized water and then added to 50 mL of ethylene glycol (EG). After stirring for 20 min, 10 mL of a solution containing 0.2015 g of NaF was dripped into the suspension under stirring. After additional agitation for 10 min, the as-obtained mixture was transferred into a 100 mL autoclave and heated at 180 °C for 12 h. After the autoclave was naturally cooled to room temperature, the precipitate was separated by centrifugation, washed with deionized water and ethanol in sequence, and then dried in air at 60 °C for 12 h. Hollow $NaYF_4$:Yb/Er microspheres were obtained. After calcination at 550 °C for 3 h, α-$NaYF_4$:Yb/Er hollow microspheres were achieved.

Preparation of Drug Storage/Release System. In a modified process,[61] 30 mg of as-prepared α-$NaYF_4$:Yb/Er hollow microspheres was dispersed in 5 mL of phosphate buffer solution (PBS, pH = 7.4) with a DOX concentration of 0.5 mg/mL. The mixture was shaken for 24 h at room temperature to reach the equilibrium state in dark

dx.doi.org/10.1021/ic4001818 | Inorg. Chem. 2013, 52, 9184−9191

condition. Then the solution was centrifuged to collect the DOX-loaded $NaYF_4$:Yb/Er sample, which is denoted as DOX-$NaYF_4$:Yb/Er. The supernatant solution was collected, and the content of residual DOX was determined by UV−vis measurement at a wavelength of 480 nm, as shown in Figure S1, Supporting Information. The in vitro delivery test was performed by immersing the DOX-$NaYF_4$:Yb/Er sample in 10 mL of PBS under gentle stirring in dark condition, and the immersing temperature was kept at 37 °C. At a selected time interval, the buffer solution was quickly taken and replaced with an equal volume of fresh buffer solution. The amount of released DOX in the supernatant solution was measured by a UV−vis spectrophotometer. To evaluate the DOX loading amount and loading efficiency, the supernatant and washed solutions were collected and the residual DOX content (R_{DOX}) was obtained by UV−vis measurement at 480 nm. The loading efficiency of DOX can be calculated as follows: $[(O_{DOX} - R_{DOX})/O_{DOX}] \times 100\%$, where O_{DOX} is the original DOX content.

Biocompatibility Assay. The biocompatibility of α-$NaYF_4$:Yb/Er hollow microspheres was assessed by the standard 3-(4,5-dimethylthiazol-2-yl)-2,5-diphenyltetrazolium bromide (MTT) assay. In a typical procedure, 5000−6000 L929 fibroblast cells in 200 μL of media per well were plated in 96-well plate and cultured in 5% CO_2 at 37 °C for 24 h overnight to allow the cells to attach to the wells. α-$NaYF_4$:Yb/Er sample was sterilized by ultraviolet irradiation for 2 h; then serial dilutions of the particles at concentrations of 6.25, 12.5, 25, 50, 100, and 200 μg/mL were added to the culture wells to replace the original culture medium and incubated for another 24 h in 5% CO_2 at 37 °C. A 5 mg/mL amount of a stock solution of MTT was prepared in PBS, and 20 μL of this stock solution was added to each well containing different amounts of $NaYF_4$:Yb/Er and incubated for another 4 h. During this period, viable cells reduce MTT to formazan pigment, which can be dissolved by dimethyl sulfoxide (DMSO). After incubation, 100 μL of acidified isopropanol was added to each well and placed on a shaking table (150 rpm, 5 min) to thoroughly mix the formazan into the solvent. The absorbance of the suspension was recorded under a microplate reader at 570 nm.

Characterization. X-ray powder diffraction (XRD) was examined on a Rigaku D/max-TTR-III diffractometer at a scan rate of 10°/min in the 2θ range from 10° to 80° using Cu Kα radiation (λ = 0.15405 nm). The morphology and composition of the as-prepared samples were inspected on a scanning electron microscope (SEM, JSM-6480A, Japan Electronics) equipped with an energy-dispersive X-ray spectrum (EDS, INC250, Japan Electronic). Transmission electron microscopy (TEM) and high-resolution transmission electron microscopy (HRTEM) were performed on a FEI Tecnai G^2 S-Twin transmission electron microscope with a field emission gun operating at 200 kV to elucidate the dimensions and structural details of the particles. N_2 adsorption/desorption isotherms were measured at a liquid nitrogen temperature (−196 °C) using a Micromeritics ASAP 2010 M instrument. The specific surface area was determined by the Brunauer−Emmett−Teller (BET) method. Fourier transform infrared spectroscopy (FT-IR) spectra were recorded with a Perkin-Elmer 580B infrared spectrophotometer using the KBr pellet technique. Thermogravimetric analysis (TGA) was carried out on a Netzsch STA 409 thermoanalyzer with a heating rate of 5 °C/min. UC emission spectra were obtained using 980 nm LD Module (K98D08M-30W, China) as the excitation source and detected by R955 (HAMAMATSU) from 400 to 900 nm. UV−vis absorption spectra were obtained on a UV-1601 spectrophotometer. All of the measurements were performed at room temperature.

RESULTS AND DISCUSSION

Phase, Structure, and Morphology. Figure 1 shows the XRD patterns of MF@$Y(OH)CO_3$:Yb/Er microspheres and $NaYF_4$:Yb/Er hollow microspheres with or without calcination, respectively. It is found that no obvious diffraction peak appears in Figure 1A, which indicates that the as-formed MF@$Y(OH)CO_3$:Yb/Er is amorphous via a urea-based homogeneous precipitation method. The component of the amorphous

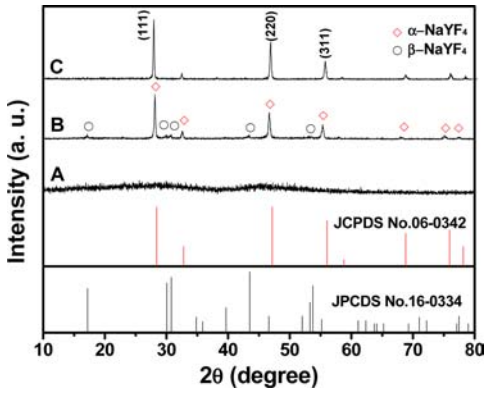

Figure 1. XRD patterns of (A) MF@$Y(OH)CO_3$:Yb/Er, (B) $NaYF_4$:Yb/Er hollow microspheres, and (C) α-$NaYF_4$:Yb/Er hollow microspheres after calcination at 550 °C for 3 h. Standard data for cubic $NaYF_4$ (JCPDS No. 06-0342) and hexagonal $NaYF_4$ (JCPDS No.16-0334) are presented for comparison.

precursor before solvothermal reaction has been confirmed to be $Y_{0.8}Yb_{0.18}Er_{0.02}(OH)CO_3$ on the basis of a previous report and the XRD pattern and SEM image provided in the Supporting Information (Figures S2 and S3).[62] When the precursor reacted with NaF at 180 °C for 12 h in the solvothermal process, the diffraction peaks of as-synthesized product can be indexed to the mixed phase of α- and β-$NaYF_4$ (Figure 1B), and both the intensity and position of (111), (220), and (311) diffraction peaks can be assigned to the α phase. Thereby, α-$NaYF_4$ is predominant. To further determine the chemical composition of the product, the sample was calcined at 550 °C for 3 h. It is well known that $Y(OH)CO_3$ will be thermally decomposed into Y_2O_3 after annealing at 550 °C. While the XRD pattern of the calcined sample (Figure 1C) indicates that the peaks can be well indexed to pure cubic $NaYF_4$ phase (JCPDS No. 06-0342), no diffraction peaks of Y_2O_3 can be found, revealing $Y(OH)CO_3$ precursor was completely converted into mixed phase $NaYF_4$ through the solvothermal process and further converted into pure α-$NaYF_4$ after calcination.

As shown in the SEM image of MF microspheres (Figure 2A), the MF template consists of uniform microspheres with an average diameter of 2.2 μm. The magnified SEM image (Figure 2B) reveals that MF microspheres have very smooth surfaces. In Figure 2C for MF@$Y(OH)CO_3$:Yb/Er microspheres, the sample inherits the spherical shape and good dispersion of the MF cores. The surfaces are much rougher than those of bare MF cores due to precipitation of the $Y(OH)CO_3$:Yb/Er layer, which can be clearly confirmed by the magnified SEM image (Figure 2D). In the TEM image for MF@$Y(OH)CO_3$:Yb/Er (Figure 2E), the apparent contrast between the core and the shell directly evidence the core−shell structure. As shown in the magnified TEM image (Figure 2F), the average size of MF@$Y(OH)CO_3$:Yb/Er microspheres and the shell is about 2.4 μm and 190 nm, respectively.

From the SEM images of α-$NaYF_4$:Yb/Er hollow microspheres (Figure 3A and 3B), we can see that the as-prepared $NaYF_4$:Yb/Er is composed of uniform microspheres with narrow size distribution. In addition, the average size of α-$NaYF_4$:Yb/Er hollow microspheres is about 2.2 μm. It should be noted that the hollow structure can be clearly observed from the broken particle (inset in Figure 3B). The hollow structure is also confirmed by the TEM image, as shown in Figure 3C. In

dx.doi.org/10.1021/ic4001818 | Inorg. Chem. 2013, 52, 9184−9191

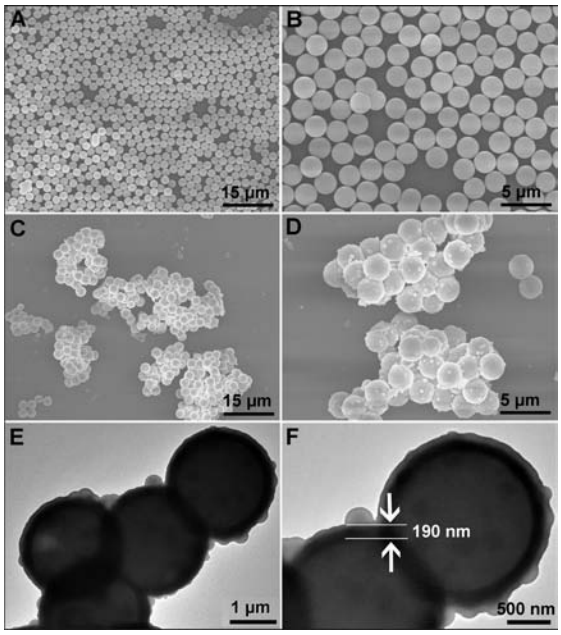

Figure 2. Low- (A) and high-magnification (B) SEM images of pure MF colloidal microspheres, low- (C) and high-magnification (D) SEM images of MF@$Y(OH)CO_3$:Yb/Er microspheres, and low- (E) and high-magnification (F) TEM images of MF@$Y(OH)CO_3$:Yb/Er microspheres.

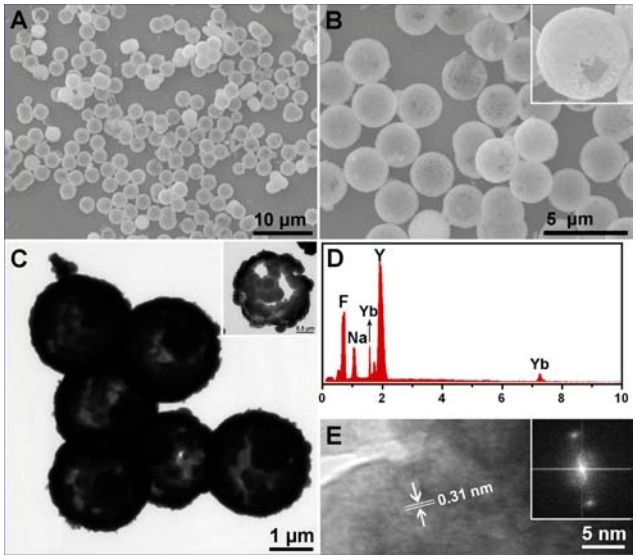

Figure 3. Low- (A) and high-magnification (B) SEM images of α-$NaYF_4$:Yb/Er hollow microspheres; (inset) enlarged single hollow microsphere with open pore. (C) TEM image of α-$NaYF_4$:Yb/Er hollow microspheres. (D) EDS of α-$NaYF_4$:Yb/Er hollow microspheres. (E) HRTEM image of α-$NaYF_4$:Yb/Er hollow microspheres; (inset) corresponding fast Fourier transform (FFT) image.

addition, the hollow structures possess large voids inside the shells and small pores or broken holes at the shells. The average diameter (2.2 μm) of the $NaYF_4$ hollow microspheres with rough surfaces is slightly decreased in comparison with that of the MF@$Y(OH)CO_3$:Yb/Er precursor (2.4 μm). It is believed that the shrinkage is caused by conversion from the loosely ranged $Y(OH)CO_3$:Yb/Er precursor to the relatively compact $NaYF_4$:Yb/Er layer and dissolving of the MF templates. EDS (Figure 3D) confirms the presence of Na, Y, F, and Yb elements in the hollow structure, and no oxygen element is detected, confirming complete transformation from $Y(OH)CO_3$:Yb/Er to $NaYF_4$:Yb/Er. In the HRTEM image (Figure 3E), the distance of 0.31 nm between the adjacent lattice fringes of $NaYF_4$:Yb/Er hollow microspheres matches well with the d_{110} spacing (0.314 nm) of cubic $NaYF_4$ (JCPDS No. 06-0342). This is also supported by the fast Fourier transform (FFT) pattern (inset in Figure 3E), which shows diffraction spots of the (110) planes of α-$NaYF_4$ and also reveals the single-crystalline nature of the sample.

Figure 4 gives the N_2 adsorption/desorption isotherm and pore size distribution of α-$NaYF_4$:Yb/Er hollow microspheres.

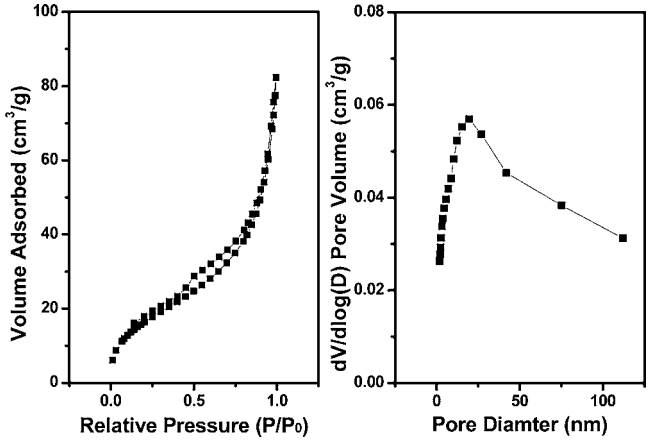

Figure 4. N_2 adsorption/desorption isotherm (left) and pore size distribution (right) of α-$NaYF_4$:Yb/Er hollow microspheres.

We can see that the sample shows a typical IV-typed isotherm with a H1-hysteresis loop, which are related with the typically mesoporous structure. The BET surface area and total pore volume are calculated to be 49 m^2/g and 0.128 cm^3/g, respectively. Notably, the pore sizes are mainly due to the small pores or broken holes in the shells formed during the solvothermal process, which is also confirmed by the SEM and TEM images (Figure 3).

Figure S4, Supporting Information, shows the TG curves of the MF@$Y(OH)CO_3$:Yb/Er microspheres and α-$NaYF_4$:Yb/Er hollow microspheres, respectively. As shown, weight loss can be observed before 100 °C, which may be caused by the absorbed water on the surface of the samples. For MF@$Y(OH)CO_3$:Yb/Er, the two rapid weight losses can be assigned to dehydration and burning of MF template from 100 to 550 °C and conversion from amorphous precursor to crystalline Y_2O_3 between 550 and 800 °C. In addition, the total weight loss is about 67.1%. As for α-$NaYF_4$:Yb/Er hollow structure, only a weight loss of 3.7% from 100 to 550 °C indicates that MF template has been effectively removed during the solvothermal process. From 550 to 800 °C we can hardly find the weight loss, indicating that no $Y(OH)CO_3$:Yb/Er exists in $NaYF_4$ hollow microspheres, which agrees with the XRD result.

FT-IR spectra are used to identify the functional groups of the MF template, MF@$Y(OH)CO_3$:Yb/Er microspheres, and α-$NaYF_4$:Yb/Er hollow microspheres (Figure S5, Supporting Information). The FT-IR spectrum of the MF template (Figure S5A, Supporting Information) shows the obvious absorption bands of OH/NH_2 (3377 cm^{-1}), NH_2 (1558, 1496, 1351 cm^{-1}), C−N (1164 cm^{-1}), C−O−C (1007 cm^{-1}), and C−N−C (811 cm^{-1}).[60] The FT-IR spectrum of MF@$Y(OH)CO_3$:Yb/

dx.doi.org/10.1021/ic4001818 | Inorg. Chem. 2013, 52, 9184−9191

Er is very similar to that of the MF template. However, the IR band of the ether group (1007 cm^{-1}) disappears, which may be caused by coating the $Y(OH)CO_3$:Yb/Er precursor onto the surface of MF microspheres. As for α-$NaYF_4$:Yb/Er hollow microspheres (Figure S5C, Supporting Information), the absorption band at 3354 cm^{-1} can also be assigned to the vibration of hydroxyl (−OH). Notably, most of the functional groups of MF template nearly disappear, revealing that the MF template can be effectively removed during the solvothermal process.[20,62,63]

Formation Process of $NaYF_4$:Yb/Er Hollow Microspheres. On the basis of above experimental results, a general schematic illustration of the formation process of α-$NaYF_4$:Yb/Er hollow microspheres is proposed in Scheme 1. First,

Scheme 1. Schematic Illustration of the Formation Process for α-$NaYF_4$:Yb/Er Hollow Microspheres

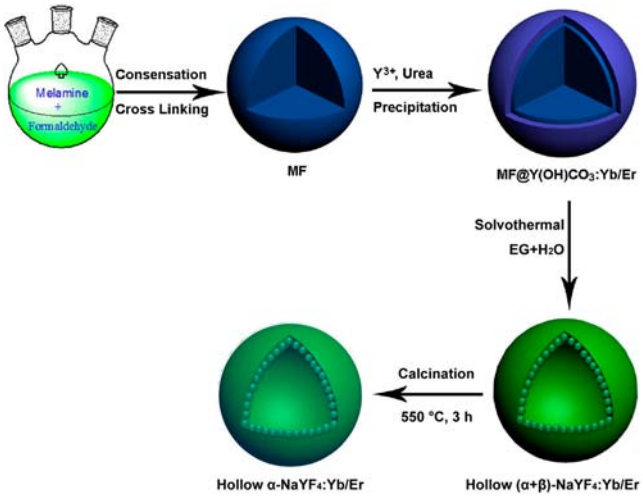

monodisperse colloid MF microspheres were prepared, which will act as the hard template. Then, MF@$Y(OH)CO_3$:Yb/Er precursor was fabricated via a urea-based homogeneous precipitation route on the surfaces of colloidal MF spheres. Then $Y(OH)CO_3$:Yb/Er layer was transformed into $NaYF_4$:Yb/Er with the mixed phase of α and β by a subsequent solvothermal process, and MF cores were dissolved in the solvent simultaneously. This process can be described as follows: the Y^{3+} (Yb^{3+}, Er^{3+}) ions ionized from the precursor react with Na^+ and F^- in the solution to form $NaYF_4$:Yb/Er layer on the surface of MF microspheres; meanwhile, MF microspheres are dissolved in the organic solvent under high temperature and pressure. Finally, pure α-$NaYF_4$:Yb/Er hollow microspheres are obtained by a subsequent calcination process.

Upconversion Photoluminescence Properties. $NaYF_4$ has proved to be an efficient host lattice for downconversion and upconversion processes due to the lower phonon energies.[64−66] Here, we select Yb^{3+}- and Er^{3+}-codoped ions to investigate the UC emission properties of the hollow structured product. Figure 5 shows the upconversion spectrum of α-$NaYF_4$:Yb/Er hollow microspheres under 980 nm laser LD excitation. It is found that two primary bands in the green emission region with maxima at 521 and 543 nm can be assigned to the $^2H_{11/2} \rightarrow {}^4I_{15/2}$ and $^4S_{3/2} \rightarrow {}^4I_{15/2}$ transitions of the Er^{3+} ions, and a weak band at about 651 nm is attributable to the $^4F_{9/2} \rightarrow {}^4I_{15/2}$ transition of Er^{3+} ions. The chromaticity coordinates are $x = 0.272$ and $y = 0.661$, locating in the green region, which corresponds to the photograph under 980 nm irritation (inset in Figure 5A). The excitation power-dependent UC green and red emissions of α-$NaYF_4$:Yb/Er hollow microspheres are presented in Figure 5B. It is well known that the output UC luminescent intensity (I_{UC}) is proportional to the infrared excitation power (I_{IR}) as $I_{UC} \propto I_{IR}^n$, where n is the absorbed photon numbers per emitted visible photon; its value is obtained from the slope of the fitted line of the plot of log (I_{UC}) versus log (I_{IR}). As shown in Figure 5B, the respective slope of the linear fits of log (I_{UC}) versus log (I_{IR}) for the green and red emissions in α-$NaYF_4$:Yb/Er sample is 1.91 and 1.72, indicating that two photons are involved to produce the green and red UC emissions. The result is in good agreement with previous reports for other Yb^{3+}/Er^{3+}-doped fluorides. The UC energy transfer process upon 980 nm LD excitation based on above result is proposed in Figure 5C. It can be seen that the green and red emissions all need a two-photon process to populate the $^2H_{11/2}/{}^4S_{3/2}$ or $^4F_{9/2}$ level. First, the ground state electrons are excited to the $^4I_{11/2}$ intermediate state of the Er^{3+} ion and then to the $^4F_{7/2}$ state via a successive transfer of energy from Yb^{3+} ($^2F_{5/2}$ excited state). Subsequently, those electrons nonradiatively decay to the lower $^2H_{11/2}$ and $^4S_{3/2}$ excited state energy levels, respectively. After these electrons return to the ground state again, it gives the green emission. Alternatively, the electron can further relax and populate the $^4F_{9/2}$ level. Subsequent radiative relaxation from the $^4F_{9/2}$ level of the Er^{3+} ion to the ground state $^4I_{15/2}$ level leads to the red emission.

Drug Loading, Release Properties, and Biocompatibility. As a typical antitumor drug, DOX was selected to evaluate the release behavior from drug-loaded $NaYF_4$:Yb/Er system. In the DOX loading process, the DOX molecules are entrapped within the hollow structure by an impregnation process. The drug loading amount is determined to be 23.2 μg/mg (DOX/$NaYF_4$:Yb/Er), and the loading efficiency is 27.8 wt % at pH = 7.4.

Figure 6 shows the in vitro release profiles of DOX from DOX-$NaYF_4$:Yb/Er systems in PBS buffer solutions with different pH values at 37 °C. We find a relatively fast release within the first 1.5 h followed by a sustained release over 12 h. The initial fast release can be assigned to rapid diffusion of the physically adsorbed drug molecules weakly adsorbed on the outer surfaces or near the pore entrances. Then the drug adsorbed in the inner surfaces or channels of the pores by strong interaction between drug molecules and the hydrogen bonds on the material surface will dissolve in a sustained manner. Furthermore, to inhibit tumor cell growth in tumor treatment, the initial burst DOX release is preferable to achieve sufficient initial dosage of the antitumor drug. For the cancer cells that survive the initial stage of drug release, the sustained DOX release is necessary to prevent their further proliferation. Thus, the drug release performance of the carrier makes it a promising candidate for tumor therapy.

Notably, the carrier exhibits obvious pH-dependent release properties in different pH solutions, which may be explained by the fact that with the decrease of the pH value the potential of the particle surface becomes more positive, thus weakening the electrostatic adsorption force with positively charged DOX molecules, leading to faster drug release. Considering the various pH values at different body sites and especially that cancer tissue is acidic extracellular, the pH-sensitive carrier can be used to control the release of drug, which is beneficial to targeting cancerous tissues and reducing toxic side effects for normal tissues. Thus, this carrier with pH-dependent release

dx.doi.org/10.1021/ic4001818 | Inorg. Chem. 2013, 52, 9184−9191

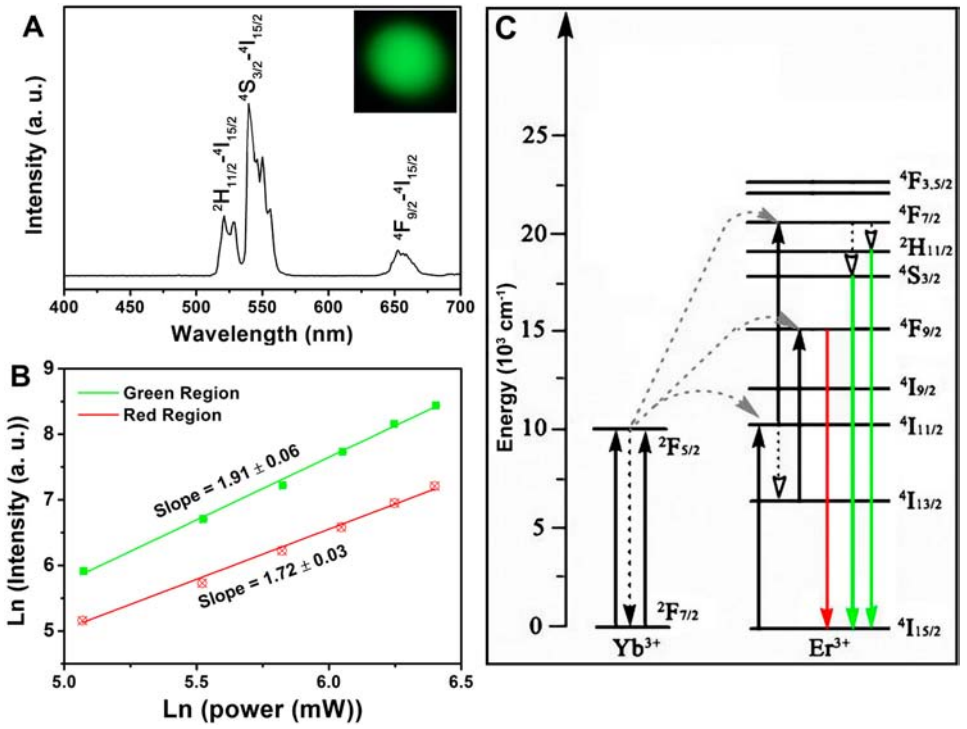

Figure 5. (A) Upconversion emission spectrum of α-$NaYF_4$:Yb/Er hollow microspheres under 980 nm LD excitation, (B) pump power dependence of the green and red upconverted emissions under 980 nm LD excitation, and (C) proposed energy transfer mechanism in Yb^{3+}/Er^{3+}-doped α-$NaYF_4$ hollow microspheres. Inset in A is the luminescent photograph of the sample under 980 nm irradiation.

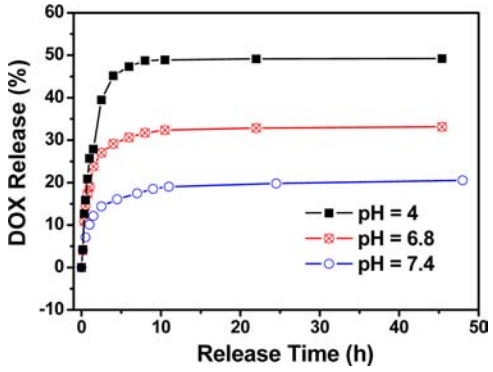

Figure 6. Cumulative DOX release from DOX-$NaYF_4$:Yb/Er system in PBS buffers with different pH values.

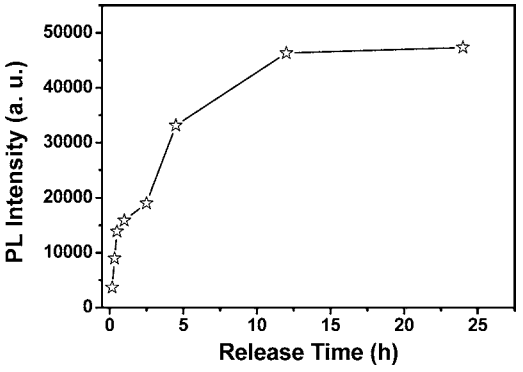

Figure 7. UC emission intensity of Er^{3+} in DOX-loaded α-$NaYF_4$:Yb/Er as a function of release time.

properties should have high potential as a smart carrier for releasing antitumor drug by changing the pH environment.

The UC emission intensity of a DOX-loaded $NaYF_4$:Yb/Er system as a function of release time (the cumulative released amount of DOX) at a pH value of 7.4 is given in Figure 7 and Figure S6A, Supporting Information. As shown, the emission intensity (the integrated green and red emissions) of the system strongly depends on the amount of released DOX. It is well known that emission of rare-earth ions will be quenched to some extent in environments which contain high phonon frequency.[67] (For example, emission of Eu^{3+} will be seriously quenched by OH groups with a vibrational frequency near 3450 cm^{-1}.) The emission intensity is greatly quenched by the loaded DOX with high-frequency phonon vibrations (1000–3450 cm^{-1}) and increases with the released DOX, achieving its maximum when the release process is completely stopped. The gradually weakened quenching effect due to the released DOX yields the increase of emission intensity. The result suggests the potential of this functional carrier to be tracked or monitored during the release process. In addition, MTT assay (Figure S7, Supporting Information) demonstrates the satisfactory biocompatibility of the sample in all dosages, indicating that the nontoxic property of the sample and therefore is promising as drug carrier.

CONCLUSIONS

In summary, we reported a two-step and accurate route for fabrication of highly uniform α-$NaYF_4$:Yb/Er hollow microspheres with an average diameter of 2.2 μm using core–shell structured MF@Y $(OH)CO_3$:Yb/Er microspheres as template, followed by the solvothermal and calcination processes. It is worthy to note that MF spheres were directly dissolved in the organic solvent under hydrothermal environment without additional calcination and leaching process. The as-prepared α-$NaYF_4$:Yb/Er hollow microspheres exhibit the characteristic

dx.doi.org/10.1021/ic4001818 | Inorg. Chem. 2013, 52, 9184–9191

green UC emissions of Er^{3+} under the 980 nm LD excitation. Furthermore, this hollow structured material demonstrates good biocompatibility, sustained DOX release properties, and potential tracked/monitored properties, which are have high potential in the biomedical field.

■ ASSOCIATED CONTENT

Ⓢ Supporting Information

This material is available free of charge via the Internet at http://pubs.acs.org.

■ AUTHOR INFORMATION

Corresponding Author

*E-mail: gaishili@hrbeu.edu.cn (S.G.), yangpiaoping@hrbeu.edu.cn (P.Y.).

Notes

The authors declare no competing financial interest.

■ ACKNOWLEDGMENTS

Financial support from the National Natural Science Foundation of China (NSFC 21271053), Research Fund for the Doctoral Program of Higher Education of China (20112304110021), Program for New Century Excellent Talents in University, Natural Science Foundation of Heilongjiang Province (LC2012C10), Harbin Sci.-Tech. Innovation Foundation (RC2012XK017012), and Fundamental Research Funds for the Central Universities of China is greatly acknowledged.

■ REFERENCES

(1) Yang, P. P.; Gai, S. L.; Lin, J. *Chem. Soc. Rev.* **2012**, *41*, 3679.
(2) Sun, Y.; Xia, Y. *Science* **2002**, *298*, 2176.
(3) Yin, Y.; Rioux, R. M.; Erdonmez, C. K.; Hughes, S.; Somorja, G. A.; Alivisatos, A. P. *Science* **2004**, *304*, 711.
(4) Yang, H. G.; Zeng, H. C. *Angew. Chem., Int. Ed.* **2004**, *43*, 5930.
(5) Yang, J.; Qi, L.; Lu, C.; Ma, J.; Cheng, H. *Angew. Chem., Int. Ed.* **2005**, *44*, 598.
(6) Chen, J.; Saeki, F.; Wiley, B. J.; Cang, H.; Cobb, M. J.; Li, Z. Y.; Au, L.; Zhang, H.; Kimmey, M. B.; Li, X.; Xia, Y. *Nano Lett.* **2005**, *5*, 473.
(7) Wei, W.; Ma, G. H.; Hu, G.; Yu, D.; Mcleish, T.; Du, Z. G.; Shen, Z. Y. *J. Am. Chem. Soc.* **2008**, *130*, 15808.
(8) Zhao, W. R.; Chen, H. R.; Li, Y. S.; Li, L.; Lang, M. D.; Shi, J. L. *Adv. Funct. Mater.* **2008**, *18*, 2780.
(9) Feng, Z.; Li, Y.; Niu, D.; Li, L.; Zhao, W.; Chen, H.; Li, L.; Gao, J.; Ruan, M.; Shi, J. *Chem. Commun.* **2008**, 2629.
(10) Zhu, Y.; Shi, J.; Shen, W.; Chen, H.; Dong, X.; Ruan, M. *Nanotechnology* **2005**, *16*, 2633.
(11) Liu, J.; Hartono, S. B.; Jin, Y.; Li, Z.; Lu, G.; Qiao, S. *J. Mater. Chem.* **2010**, *20*, 4595.
(12) Guo, L.; Liang, F.; Wen, X.; Yang, S.; He, L.; Zheng, W.; Chen, C.; Zhong, Q. *Adv. Funct. Mater.* **2007**, *17*, 425.
(13) Hou, H.; Peng, Q.; Zhang, S.; Guo, Q.; Xie, Y. *Eur. J. Inorg. Chem.* **2005**, 2625.
(14) Wang, W.; Zhang, P.; Peng, L.; Xie, W.; Zhang, G.; Tu, Y.; Mai, W. *CrystEngComm* **2010**, *12*, 700.
(15) Wang, J.; Xia, Y.; Wang, W.; Mokaya, R.; Poliakoff, M. *Chem. Commun.* **2005**, 210.
(16) Yang, Z.; Cong, H.; Cao, W. *J. Polym. Sci., Part A: Polym. Chem.* **2004**, *42*, 4284.
(17) Chen, I. H.; Wang, C.-C.; Chen, C.-Y. *Scr. Mater.* **2008**, *58*, 37.
(18) Guo, X.-F.; Kim, Y.-S.; Kim, G.-J. *J. Phys. Chem. C* **2009**, *113*, 8313.
(19) Wang, L. Z.; Ebina, Y.; Takada, K.; Sasaki, T. *Chem. Commun.* **2004**, 1074.
(20) Jia, G.; You, H.; Liu, K.; Zheng, Y.; Guo, N.; Zhang, H. *Langmuir* **2010**, *26*, 5122.
(21) Liu, G.; Hong, G. *J. Solid State Chem.* **2005**, *178*, 1647.
(22) Zhang, K.; Zhang, X.; Chen, H.; Chen, X.; Zheng, L.; Zhang, J.; Yang, B. *Langmuir* **2004**, *20*, 11312.
(23) Kim, H.; Cho, J. *Chem. Mater.* **2008**, *20*, 1679.
(24) Ma, Y.; Qi, L.; Ma, J.; Cheng, H.; Shen, W. *Langmuir* **2003**, *19*, 9079.
(25) Strandwitz, N. C.; Stucky, G. D. *Chem. Mater.* **2009**, *21*, 4577.
(26) Yang, R.; Li, H.; Qiu, X.; Chen, L. *Chem.—Eur. J.* **2006**, *12*, 4083.
(27) Chen, J.-F.; Ding, H.-M.; Wang, J.-X.; Shao, L. *Biomaterials* **2004**, *25*, 723.
(28) Zheng, X.; Liu, C.; Xie, Y. *Eur. J. Inorg. Chem.* **2006**, 2364.
(29) Meiser, F.; Cortez, C.; Caruso, F. *Angew. Chem., Int. Ed.* **2004**, *43*, 5954.
(30) Hao, J. H.; Zhang, Y.; Wei, X. H. *Angew. Chem., Int. Ed.* **2011**, *50*, 6876.
(31) Li, Z. Q.; Zhang, Y.; Jiang, S. *Adv. Mater.* **2008**, *20*, 4765.
(32) Hu, H.; Yu, M. X.; Li, F. Y.; Chen, Z. G.; Gao, X.; Xiong, L. Q.; Huang, C. H. *Chem. Mater.* **2008**, *20*, 7003.
(33) Johnson, N. J. J.; Korinek, A.; Dong, C. H.; van Veggel, F. C. J. M. *J. Am. Chem. Soc.* **2012**, *134*, 11068.
(34) Wang, Z. L.; Hao, J. H.; Chan, H. L. W.; Law, G. L.; Wong, W. K.; Wong, K. L.; M. Murphy, B.; Su, T.; Zhang, Z. H.; Zeng, S. Q. *Nanoscale* **2011**, *3*, 2175.
(35) Wang, F.; Deng, R. R.; Wang, J.; Wang, Q. X.; Han, Y.; Zhu, H. M.; Chen, X. Y.; X. Liu, G. *Nat. Mater.* **2011**, *10*, 968.
(36) Liu, Y. S.; Tu, D. T.; Zhu, H. M.; Li, R. F.; Luo, W. Q.; Chen, X. Y. *Adv. Mater.* **2010**, *22*, 3266.
(37) Zhou, J. C.; Yang, Z. L.; Dong, W.; Tang, R. J.; Sun, L. D.; Yan, C. H. *Biomaterials* **2012**, *32*, 9059.
(38) Ju, Q.; Tu, D. T.; Liu, Y. S.; Li, R. F.; Zhu, H. M.; Chen, J. C.; Chen, Z.; Huang, M. D.; Chen, X. Y. *J. Am. Chem. Soc.* **2012**, *134*, 1323.
(39) Diamente, P. R.; Raudsepp, M.; van Veggel, F. C. J. M. *Adv. Funct. Mater.* **2007**, *17*, 363.
(40) Tu, D. T.; Liu, L. Q.; Ju, Q.; Liu, Y. S.; Zhu, H. M.; Li, R. F.; Chen, X. Y. *Angew. Chem. Inter. Ed.* **2011**, *50*, 6306.
(41) Burns, J. H. *Inorg. Chem.* **1965**, *6*, 881.
(42) Wang, F.; Liu, X. G. *J. Am. Chem. Soc.* **2008**, *130*, 5642.
(43) Li, Z. Q.; Zhang, Y. *Angew. Chem., Int. Ed.* **2006**, *45*, 7732.
(44) Li, Z. Q.; Zhang, Y.; Jiang, S. *Adv. Mater.* **2008**, *20*, 4765.
(45) Kramer, K. W.; Biner, D.; Frei, G.; Gudel, H. U.; Hehlen, M. P.; Luthi, S. R. *Chem. Mater.* **2004**, *16*, 1244.
(46) Li, C. X.; Quan, Z. W.; Yang, J.; Yang, P. P.; Lin, J. *Inorg. Chem.* **2007**, *46*, 6349.
(47) Liang, X.; Wang, X.; Zhuang, J.; Peng, Q.; Li, Y. D. *Inorg. Chem.* **2007**, *46*, 6050.
(48) Wang, L. Y.; Li, Y. D. *Chem. Mater.* **2007**, *19*, 727.
(49) Li, C. X.; Lin, J. *J. Mater. Chem.* **2010**, *20*, 6831.
(50) Wang, X.; Zhuang, J.; Peng, Q.; Li, Y. D. *Inorg. Chem.* **2006**, *45*, 6661.
(51) Wang, Z. L.; Hao, J. H.; Chan, H. L. W. *J. Mater. Chem.* **2010**, *20*, 3178.
(52) Zeng, J. H.; Su, J.; Li, Z. H.; Yan, R. X.; Li, Y. D. *Adv. Mater.* **2005**, *17*, 2119.
(53) Auzel, F. *Chem. Rev.* **2004**, *104*, 139.
(54) Heer, S.; Kompe, K.; Gudel, H. U.; Haase, M. *Adv. Mater.* **2004**, *16*, 2102.
(55) Yi, G. S.; Lu, H. C.; Zhao, S. Y.; Yue, G.; Yang, W. J. *Nano Lett.* **2004**, *4*, 2191.
(56) Boyer, J.-C.; Vetrone, F.; Cuccia, L. A.; Capobianco, J. A. *J. Am. Chem. Soc.* **2006**, *128*, 7444.
(57) Mai, H. X.; Zhang, Y. W.; Si, R.; Yan, Z. G.; Sun, L. D.; You, L. P.; Yan, C. H. *J. Am. Chem. Soc.* **2006**, *128*, 6426.
(58) Zhang, F.; Shi, Y. F.; Sun, X. H.; Zhao, D. Y.; Stucky, G. D. *Chem. Mater.* **2009**, *21*, 5237.

(59) Yang, D. M.; Kang, X. J.; Ma, P. A.; Dai, Y. L.; Hou, Z. Y.; Cheng, Z. Y.; Li, C. X.; Lin, J. *Biomaterials* **2013**, *34*, 1601.
(60) Friedel, B.; Greulich-Weber, S. *Small* **2006**, *2*, 859.
(61) Gai, S. L.; Yang, P. P.; Ma, P. A.; Wang, D.; Li, C. X.; Li, X. B.; Niu, N.; Lin, J. *J. Mater. Chem.* **2011**, *21*, 16420.
(62) Jia, G.; You, H.; Song, Y.; Huang, Y.; Yang, M.; Zhang, H. *Inorg. Chem.* **2010**, *49*, 7721.
(63) Yang, P. P.; Gai, S. L.; Liu, Y. C.; Wang, W. X.; Li, C. X.; Lin, J. *Inorg. Chem.* **2011**, *50*, 2182.
(64) Auzel, F. *Chem. Rev.* **2004**, *104*, 139.
(65) Zhou, J.; Liu, Z.; Li, F. Y. *Chem. Soc. Rev.* **2012**, *41*, 1323.
(66) Wang, G. F.; Peng, Q.; Li, Y. D. *Acc. Chem. Res.* **2011**, *44*, 322.
(67) Blasse, G.; Grabmaier, B. C. *Luminescent Materials*; Springer: Berlin, 1994; Chapter 4.

dx.doi.org/10.1021/ic4001818 | *Inorg. Chem.* 2013, 52, 9184−9191